

Clusters of Galaxies: magnetic fields and nonthermal emission

H. J. Völk^a and A. M. Atoyan^{a,b}

^a*Max-Planck-Institut für Kernphysik, D-69029 Heidelberg, Germany*

^b*Yerevan Physics Institute, 375036 Yerevan, Armenia*

Abstract

The nonthermal particle content of galaxy clusters should in part have a cosmological component generated during the early starburst phase of the member galaxies. This is reviewed in the framework of a simple cluster formation model suggested previously. It implies a nonthermal energy fraction of about 10 percent for the Intracluster gas. We also propose a mechanism for the early generation of Intracluster magnetic fields in terms of Galactic Winds. It results in typical field strengths of 10^{-7} Gauss. Such comparatively weak fields are consistent with an inverse Compton origin of the excess EUV and hard X-ray emission of the Coma cluster, given the radio synchrotron emission. The required relativistic electrons must have been accelerated rather recently, less than a few billion years ago, presumably in cluster accretion shocks. This is in contrast to the hadronic nonthermal component which accumulates on cosmological time scales, and whose π^0 -decay TeV γ -ray emission is expected to be larger, or of the same order as the inverse Compton TeV emission. This γ -radiation characterizes the energetic history of cluster formation and should be observable with future arrays of imaging atmospheric Cherenkov telescopes.

1 Introduction

Clusters of galaxies are the largest gravitationally bound structures in the Universe and may confine a representative fraction of its mass. Therefore the study of their dynamical properties and radiation content should allow, amongst other things, conclusions on the relative amounts of baryonic and nonbaryonic matter in cosmology (e.g. White and Fabian, 1995, and references therein).

Another basic characteristic, also due to confinement, is the ratio of thermal to nonthermal energy in these objects. To a significant extent that ratio is established during the epoch of galaxy formation and thus preserves the energetic history of cluster formation. We shall review this topic here. The confinement

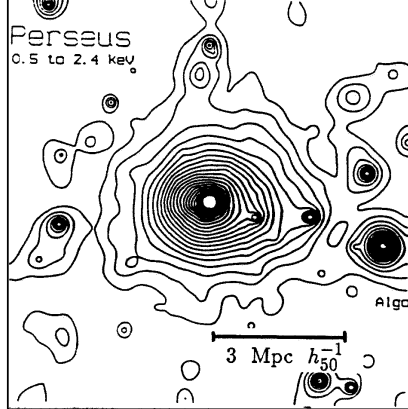


Fig. 1. Large scale contour plot of an X-ray image of the Perseus cluster from the ROSAT all sky survey (courtesy H. Böhringer).

of nonthermal particle components is intimately related to the existence of strong and chaotic magnetic fields in the intracluster medium (ICM), and we shall propose a mechanism for their early generation. This is followed by a discussion of the present-day nonthermal radiation from clusters in various wavelength ranges, in particular at very high γ -ray energies.

Rich Clusters

Rich clusters, i.e. conglomerates with typically more than 100 member galaxies, have typical radii $R_{\text{cl}} \sim$ few Mpc and baryonic masses $M_{\text{cl}} \sim 10^{14}$ to $10^{15} M_{\odot}$. The closest large cluster is the Virgo cluster at a distance of $d \sim 20$ Mpc; all the others are at a distance d of hundred Mpc and beyond. Examples for bright and relatively nearby clusters are the Perseus and the Coma clusters with $d \simeq 100$ Mpc. The Perseus cluster is the brightest cluster in soft X-rays (see Fig. 1). The large X-ray luminosity is due to the very hot ($T \sim 10^7$ to 10^8 K), massive ($M_{\text{gas}} \sim$ few $\times \sum M_{\text{gal}}$), and metal-rich ($[\text{Fe}]_{\text{cl}} \simeq 0.35 [\text{Fe}]_{\odot}$) ICM gas (e.g. Böhringer, 1996).

Apart from their primary cosmological interest, galaxy clusters also serve as extragalactic distance poles (Sunyaev-Zeldovich effect) and as gravitational telescopes for still more distant objects. This makes them important "instruments" for observational astronomy.

Cluster Formation

Most rich clusters - apart from objects still in an early formation phase, like the Virgo cluster - are characterized by a predominance of early type galaxies, i.e. elliptical (E) and lenticular (S0) galaxies which have little interstellar gas. Gas-rich spiral and irregular galaxies represent a minority. This situation is opposite to the one in the field, the space outside clusters, where the fraction of spiral galaxies is at least 75 percent. For rich clusters the metallicity of the

ICM gas, for instance in the form of the fractional ICM iron mass, is also correlated with the optical luminosity in E and S0 galaxies (Arnaud et al., 1992). The correlation supports the qualitative view that early starbursts due to galaxy-galaxy interactions of protospirals have produced a large number of Supernovae (SNe) that heated the originally present interstellar gas and generated violent Galactic Winds, leaving gas-poor E and S0 galaxies behind. This mass loss should have led ultimately to the observed strong chemical enrichment of the ICM gas. We also conjecture that the radiation and the winds from these early galaxy mergers strongly heated the remaining primordial ICM gas and thus prevented further galaxy formation. This is perhaps the physical explanation for the observed inefficiency of galaxy formation which manifests itself in the remarkable preponderance of diffuse ICM gas mass over stellar mass in clusters of galaxies.

A quantitative discussion of the dynamical prerequisites for Galactic Winds and the total number of SNe in clusters is contained in the paper by Völk et al. (1996, hereafter referred to as Paper I) which we shall summarize below.

The total number of SNe since galaxy formation in the cluster, roughly a Hubble time $T_H \simeq 1.5 \times 10^{10}$ yr ago, is given by

$$N_{\text{SN}} = \int_{-T_H}^0 dt \times \nu_{\text{SN}}(t) = \frac{0.35 [Fe]_{\odot} \times M_{\text{cl}}}{\delta M_{Fe}} ,$$

where δM_{Fe} is the amount of iron produced per event. In such starbursts we dominantly expect core collapse SNII from massive progenitor stars to occur, with $\delta M_{Fe} \simeq 0.1 M_{\odot}$ on average. For the Perseus cluster this implies $N_{\text{SN}}^{\text{Perseus}} \sim 3 \times 10^{12}$. The corresponding total energy input into the interstellar medium is $N_{\text{SN}} E_{\text{SN}} \sim 3 \times 10^{63} E_{51}$ erg, where $E_{51} = 10^{51}$ erg is the average hydrodynamic energy release per SN.

Assuming the early starbursts to occur at a typical redshift of $z \sim 2$ due to the merging of protospirals in the overdense protocluster environment (Steinmetz, 1993), with a duration of $T_{\text{SB}} \leq 10^9$ yr, we obtain

$$\frac{(N_{\text{SN}}^{\text{Perseus}} / N_{\text{gal}}^{\text{Perseus}})}{T_{\text{SB}}} \geq 100 \times \nu_{\text{SN}}^{\text{Milky Way}} .$$

Here $N_{\text{gal}}^{\text{Perseus}} \simeq 500$ denotes the number of galaxies in the cluster. As an example we can compare to the archetypical contemporary starburst galaxy M82. It has a current SN rate $\nu_{\text{SN}}^{\text{M82}} \sim 10 \times \nu_{\text{SN}}^{\text{Milky Way}}$, a wind velocity $v_{\text{wind}} \sim 2300$ km/sec, and a mass-loss rate of $\dot{M} \sim 0.8 M_{\odot}/\text{yr}$ (Breitschwerdt, 1994). The starburst nucleus of M82 is characterized by the following values for the interstellar gas temperature T , gas density n , and thermal gas pressure p : $T_{\text{base}} \sim 10^8$ K, $n_{\text{base}} \sim 0.3 \text{ cm}^{-3}$, and $p_{\text{gas}}/k_B \sim 10^7 \text{ K cm}^{-3}$ (Schaaf et al. 1989).

Since the thermal ICM gas pressure in the Perseus cluster is $p_{\text{cl}}^{\text{Perseus}}/k_B \sim 10^4 \text{ K cm}^{-3}$, it is clear that an object like M82 could readily drive a wind even against the *present-day* ICM pressure. At the galaxy formation epoch the ICM pressure was certainly much smaller than this value.

In the expanding wind flow the SN-heated gas cools adiabatically to quite small temperatures. However it is reheated in the termination shock, where the ram pressure of the wind adjusts to the ICM pressure. Beyond this point the ejected galactic gas is mixed with the unprocessed ICM gas.

Particle Acceleration

Cluster formation also implies the production of a strong nonthermal component of relativistic particles. They will be accelerated during the early phase - and possibly also in later events - and confined in the turbulent ICM medium. The confinement time generally exceeds the cluster lifetime. Thus the energy spectrum of the energetic particles is the same as that generated by their sources. In Cosmic Ray parlance these are *cosmological Cosmic Rays* (CRs).

During the early starburst particle acceleration will occur initially at the outer shocks of the Supernova Remnants (SNRs). However, like the thermal gas, this first generation of nonthermal particles will lose its energy almost completely by adiabatic cooling in the ensuing Galactic Wind.

Fresh particle acceleration will occur with high efficiency at the strong wind termination shock, at distances $\sim 100 \text{ kpc}$. The wind magnetic field will still intersect the shock at an angle $\sim 10^\circ$ (e.g. Zirakashvili et al. 1996), so that the standard process of diffusive shock acceleration approximately still works there (Fig. 2a). Assuming an overall acceleration efficiency of 10 to 30 percent, one gets a total gas internal energy $E_{\text{gas}}^{\text{GW}} \sim \text{few } 10^{62} \text{ erg}$ and a nonthermal energy $E_{\text{CR}}^{\text{GW}} \sim 10^{62} \text{ erg}$ for a system like the Perseus cluster, ultimately from star formation and subsequent SN explosions. Since the galaxies are distributed across the cluster quasi-uniformly, this will also be true for the *nonthermal particle population and the radiation* they emit. The continuing gravitational contraction/accretion of the cluster will subsequently energize CRs and thermal gas at least adiabatically, or shock accelerate/heat both components, so that finally the total energy E_{CR} of energetic particles reaches $10^{63} \text{ erg} \sim 0.1 E_{\text{gas}}$ in the cluster; E_{gas} now denotes the total internal energy of the ICM gas (Paper I). The resulting nonthermal energy density of some tenths of eV/cm^3 happens to be roughly equal to that in the interstellar medium of our Galaxy.

It is instructive to compare the expected nonthermal energy with the thermal energy content of the cluster galaxies. Assuming the stars internally to be in virial equilibrium and, for purposes of estimate, all of them to have a solar mass and radius, then $E_{\text{th}}^{\text{star}} \sim (3/10)GM_\odot^2/R_\odot \simeq 10^{48} \text{ erg}$. For a total mass of about $10^{14} M_\odot$ contained in the *galaxies* of the Perseus cluster this gives

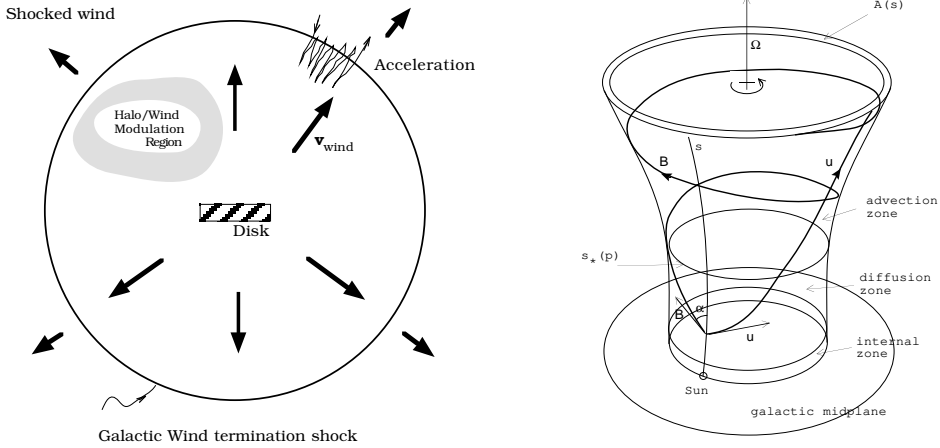


Fig. 2. **a** (left panel). Schematic of particle acceleration at a Galactic Wind termination shock. In the halo, at distances large compared to the radius of the galaxy (Disk), the wind velocity becomes radial and constant in magnitude. It goes through a strong shock transition at a distance where the ram pressure of the wind has decreased towards the external (IC) pressure. Particles injected from the heated thermal gas of the shocked wind get diffusively accelerated at this shock with high efficiency. **b** (right panel). Schematic of the flow and field configuration of an axisymmetric Galactic Wind from a rotating disk galaxy like the Milky Way, cf. Ptuskin et al. (1997). The meridional flow velocity \mathbf{u} from a circle in the disk (like that corresponding to the Sun's distance from the center of rotation) is roughly parallel to the axis of rotation to flare out at large distances. The magnetic field \mathbf{B} becomes slowly azimuthal at large meridional distances s .

a total thermal energy in stars $\sim 10^{62}$ erg, and thus $E_{\text{CR}} > \sum_{\text{gal}} \sum_{\text{stars}} E_{\text{th}}^{\text{star}}$. This means that the nonthermal ICM energy is larger than the total thermal energy of all the stars in all the galaxies contained in the cluster!

It has been argued more recently that, apart from star formation and overall gravitational contraction, also individual giant radio galaxies should have injected large and in fact comparable amounts of nonthermal particles during the life time of a cluster (Enßlin et al. 1997; Berezinsky et al. 1997). This is no doubt an important additional possibility. A weakness of this argument consists in the fact that per se it is predicated on statistical knowledge about the luminosity function for active galaxies in clusters in general, and not on direct observations of the individual cluster to which it is applied.

Particle Confinement

The large-scale magnetic field in the ICM gas may be quite chaotic and not well connected over distances exceeding typical intergalactic distances (see section 2). Thus energetic particles may not readily escape from the cluster due to such topological characteristics. However, already pure pitch angle diffusion along magnetic field lines with superposed turbulent fluctuations gives important insights into the confinement properties of galaxy clusters. Stan-

dard quasilinear theory yields a spatial diffusion coefficient κ_{\parallel} along the large scale field \mathbf{B} due to a power spectrum $P(k)$ of magnetic field fluctuations with wavelength $\lambda = 2\pi/k$ as

$$\kappa_{\parallel} = (1/3)cr_g(p) \frac{\mathbf{B}^2}{\int_k^{\infty} dk' P(k')},$$

where p denotes particle momentum, $kr_g(p) \simeq 1$, and k denotes wavenumber of the field fluctuations. Let us assume a relative fluctuation field strength of order unity at the inter-galaxy distance $1/k_0$, i.e. a totally turbulent field $P(k_0) \times k_0 \sim \mathbf{B}^2$ on this scale, and a power law form of $P(k) = P(k_0)(k/k_0)^{-n}$. Then the diffusion time across the cluster $T_{\text{esc}} \sim R_{\text{cl}}^2/\kappa_{\parallel} > T_H$ for $(cp)_{\text{protons}} \leq 10^{17} \text{ eV}$ and $\leq 10^{15} \text{ eV}$, for $n = 3/2$ and $n = 5/3$, respectively (Paper I). Also $t_{\text{loss}}^{\text{protons}} \gg T_H$ for nuclear collisions in the ICM gas. Therefore (except at sub-relativistic energies with their prevailing Coulomb losses), up to these energies CR hadrons accumulate in the cluster since the galaxy formation epoch, and that is what we called *cosmological* CRs before. The situation is different for relativistic electrons, which suffer radiative losses: energetic electrons observed now must either be secondaries or be rather recently accelerated.

2 Intracluster Magnetic Fields

The large magnetic field strengths of $B \sim 1 \mu\text{G}$ in the IC medium of rich clusters, in particular as observed by Faraday rotation measurements (e.g. Kronberg 1994), are not easily explained by a contemporary mechanism because present day turbulent dynamo effects in such a large-scale system should be extremely slow. Therefore we suggest here a field configuration that is due to the early formation history of galaxy clusters and that should be essentially preserved to this day. It should even be still in a state of development at the present epoch. The argument derives from the violent early Galactic Winds which accompany the starbursts responsible for the predominance of the early type galaxies in rich clusters.

We assume first of all that the protospirals, whose mergers constitute the building blocks for the E and S0 galaxies, had already generated galactic magnetic fields of μG strength. This should indeed be possible within about 10^8 yr , i.e. of the order of a rotation period of our Galaxy, from turbulent dynamo action that invokes buoyancy effects from CRs and magnetic reconnection on spatial scales of $O(100\text{pc})$ (Parker, 1992); such a time scale and the resulting field strengths correspond to generally accepted numbers. In the second stage the ensuing Galactic Winds extend these fields from the interacting galaxies to almost intergalactic distances. In the final and by far longest stage, that lasts until now, the fields are recompressed by the contraction of the cluster to its

present size.

The ICM fields do not reconnect on the intergalactic scale in a Hubble time. Consequently there is no need for a continuous regeneration of these fields since their formation. However, this also implies that a topologically connected overall ICM field will on average not be formed either, and that the ICM field is chaotic on a scale smaller or equal to the present intergalactic distance.

In detail we draw on arguments we have in the past used for the field configuration in a Galactic Wind from our own Galaxy (Zirakashvili et al. 1996; Ptuskin et al. 1997). They are based on estimates of the relative amount of field line reconnection vs. the extension of galactic field lines by a wind to "infinity" (Breitschwerdt et al. 1993). The basic result was that the rates of reconnection - and thus of the formation of "Parker bubbles" leaving the galaxy by their buoyancy and allowing the generation of the disk magnetic field - and of extension of this field into the galactic Halo by the pressure forces of the wind are roughly equal. Thus both effects occur, and in the cluster galaxies, magnetic energy can be generated on the large scale of the wind at the expense of the thermal and nonthermal enthalpies produced in the starburst. The geometry of the field should roughly correspond to straight field lines out to radial distances r of the order of the starburst (SB) radius, $r_{\text{gal}}^{\text{SB}} \sim 1 \text{ kpc}$, and spherically diverging field lines beyond that. The slow rotation of the system should then lead to an azimuthal field component $\propto 1/r$ which dominates at large distances over any radial component. However, in contrast to the familiar situation in the Solar Wind equatorial plane, the axis of rotation is rather parallel than perpendicular to the flow at the base of the wind, and thus the dominance of the azimuthal field component is by no means as drastic as in the case of a stellar wind (Fig. 3).

Assuming the ICM pressure $p_{\text{cl}}(z = 2)$ at the formation stage of the early type galaxies to be roughly a factor of 10^{-2} smaller than it is at present (after gravitational compression of the ICM gas), the termination shock distance r_{sh} is found from $\rho(r_{\text{sh}}) u^2/k_B \sim 10^{-2} p_{\text{cl}}(z = 0)/k_B \sim 10^2 \text{ K/cm}^{-3}$.

For M82 analogs, but with $r_{\text{gal}}^{\text{SB}} \sim 1 \text{ kpc}$, we have $p_{\text{gas}}/k_B \sim 10^7 \text{ Kcm}^{-3}$. Thus $r_{\text{sh}}/r_{\text{gal}}^{\text{SB}} \sim p_{\text{gas}}/[10^{-2} p_{\text{cl}}(0)] \simeq 300$, and therefore

$$\frac{r_{\text{sh}}}{d_{\text{gal}}^{\text{field}}(0)/(1+z)} \simeq \frac{300 \text{ kpc}}{(2 \text{ Mpc}/3)} \simeq 0.5$$

The Wind Bubble containing the shock-heated wind gas will have a radius still exceeding r_{sh} . Thus, even though the volume of hydrodynamically unaffected ICM gas may be large enough so that the ICM gas mass exceeds the mass associated with galaxies by a factor of a few - as observed - there may be that some Wind Bubbles touch. However, at the scale of r_{sh} , reconnection with a speed between 1 and 10 percent of the Alfvén velocity is too slow to

occur over a Hubble time, even in a present-day ICM magnetic field as high as 10^{-6} G. Therefore, on average, the field structure should remain topologically disconnected until today.

The field strength $B_{\text{cl}}(z = 2)$ in the Wind Bubbles should be of the order of

$$B_{\text{cl}}(z = 2) \simeq 4B_{\text{gal}}r_{\text{gal}}^{\text{SB}}/r_{\text{sh}} \sim 10^{-2}B_{\text{gal}} \sim 10^{-8}\text{G}$$

or somewhat larger, if the field in the bubble increases in the decelerating postshock flow. The ongoing cluster contraction/accretion compresses the field to lowest order isotropically $\propto l^2$, with the scale factor

$$l \simeq [n_{\text{cl}}(0)/n_{\text{bar}}(0)]^{1/3}/(1 + z),$$

where $n_{\text{cl}}(0) \sim (10^{-3} \text{ to } 10^{-4}) \text{ cm}^{-3}$ and $z = 2$. Choosing for the present mean baryon number density the value $n_{\text{bar}} \sim 3 \times 10^{-7} \text{ cm}^{-3}$, we obtain $l \sim (2.3 \text{ to } 5)$.

Finally then, we obtain for the present-day ICM field: $B_{\text{cl}}(z = 0)/B_{\text{cl}}(z = 2) \sim (5 \text{ to } 25)$. Therefore the present-day ICM magnetic field should have a mean strength of the order of 10^{-7} G, from "primordial" seed fields, randomly directed on an intergalactic scale. Although smaller by about one order of magnitude than estimated from Faraday rotation measurements, such fields need not necessarily be unrealistic, considering that observations might emphasize regions of high magnetic fields. In addition the increase of the field in the Galactic Wind bubbles beyond their postshock value might be more than a factor of unity as assumed above. Thus we cannot exclude μG fields although they certainly are at the upper limit our estimate permits. The interpretation of recent UV data also points to small field values (see section 3).

In conclusion, there is hardly any need for a contemporary "turbulent IC dynamo". Nevertheless, the estimated CR enthalpy of $\sim 0.5 \text{ erg/cm}^3$ is essentially a free energy reservoir for a future increase in B towards a mean strength of a few μG . In the next section we consider the nonthermal radiation from clusters. In particular we shall discuss the implications of the broad-band observations for the nonthermal energy content and ICM magnetic fields.

3 Nonthermal emission

From the Coma cluster radio fluxes are measured from 10.3 MHz to 2.7 GHz (Bridle and Purton, 1968; Henning 1989; Kim et al. 1990; Giovannini et al. 1993), and at 4.85 GHz an upper flux limit was reported by Kim et al. (1990). The energy fluxes $J_{\nu} \propto \nu^{-\alpha_r}$ between 30.9 MHz and 1.4 GHz are well fitted with a power-law index $\alpha_r = 1.16$ (Bowyer & Berghöfer 1998). The data at 2.7 and 4.85 GHz fall below this extrapolation, which may indicate a steepening in

the electron spectrum (Schlickeiser et al. 1987) for Lorentz-factors $\gamma \geq 5 \times 10^4$, but can be explained also as an instrumental effect (Deiss 1997). Below we use an index $\alpha_r = 1.16$.

In the extreme ultraviolet (EUV) region, diffuse radiation between 65 and 245 eV is observed which appears in excess of the thermal fluxes of the X-ray emitting gas with $T \sim 2 \times 10^6$ K, and this radiation was initially interpreted in terms of thermal emission from a gas of lower temperature, $T \sim 8 \times 10^5$ K (Lieu et al. 1996). Subsequently, the excess EUV emission, observed in a number of clusters (e.g. Mittaz et al. 1998), was suggested to represent inverse Compton (IC) radiation (Hwang 1997; Sarazin and Lieu 1998) of low energy electrons, $\gamma \sim 300$, on the 2.7 K microwave background radiation. Also Enßlin and Biermann (1998) used this possibility to estimate lower limits to the magnetic field strength in the Coma cluster (see also Lieu et al. 1998).

Bowyer and Berghöfer (1998) have shown that the size of diffuse emission of the Coma cluster is significantly larger in radio than in EUV light. In addition, the spectral index of the energy flux $J(E)$ of the EUV emission is $\alpha_{uv} \approx 0.75$ which is significantly different from that in the radio domain. Based on these arguments, Bowyer and Berghöfer (1998) suggested that two different populations of relativistic electrons should be responsible for the radio synchrotron and the EUV IC fluxes. We shall show below that the differences in these spectral indices are quite naturally explained in terms of a single population of electrons producing both the EUV excess IC and the radio synchrotron emission which avoids the need for a 2-component model.

The characteristic synchrotron frequency produced by electrons with Lorentz factor γ in the magnetic field B is $\nu \simeq (B/1 \mu\text{G})\gamma^2 \text{Hz}$ (e.g. Ginzburg 1979). Thus in a magnetic field of $B \sim 10^{-7} \text{G}$ the production of synchrotron radiation with $\alpha_r = 1.16$ in the region from 30 MHz to 1.4 GHz requires the energy distribution of the electrons $N(\gamma) \propto \gamma^{-\alpha_e}$ to extend with an index $\alpha_e = 1 + 2\alpha_r \approx 3.3$ from $\gamma_1 \simeq 1.7 \times 10^4$ to $\gamma_2 \simeq 1.4 \times 10^5$. These Lorentz factors are smaller by a factor of 3 if $B \sim 10^{-6} \text{G}$.

For the IC process the mean energy of photons is $\epsilon \simeq (4/3)\epsilon_0 \gamma^2$, where ϵ_0 is the energy of target photons. For the 2.7 K background radiation $\epsilon_0 = 6.5 \times 10^{-4} \text{eV}$. For the production of Coma's EUV spectrum from 65 to 250 eV one therefore needs a spectral index of electrons $\alpha_e \simeq 2.5$ only in a rather narrow energy region around $\gamma_{ic} \simeq 300$. This energy is much smaller than the energy γ_1 necessary for the radio emitting electrons. Thus a scenario in which radiative losses induce a break in α_e for a single population of electrons somewhere in between γ_{ic} and γ_1 can readily account for the observed indices both in the radio and the EUV. Indeed, assuming that the spectral index of the source function of electrons in the ICM is $\alpha_{inj} = 2.3$, the IC emission of those electrons at low energies will give $\alpha_{uv} = 0.65$, which is rather close to

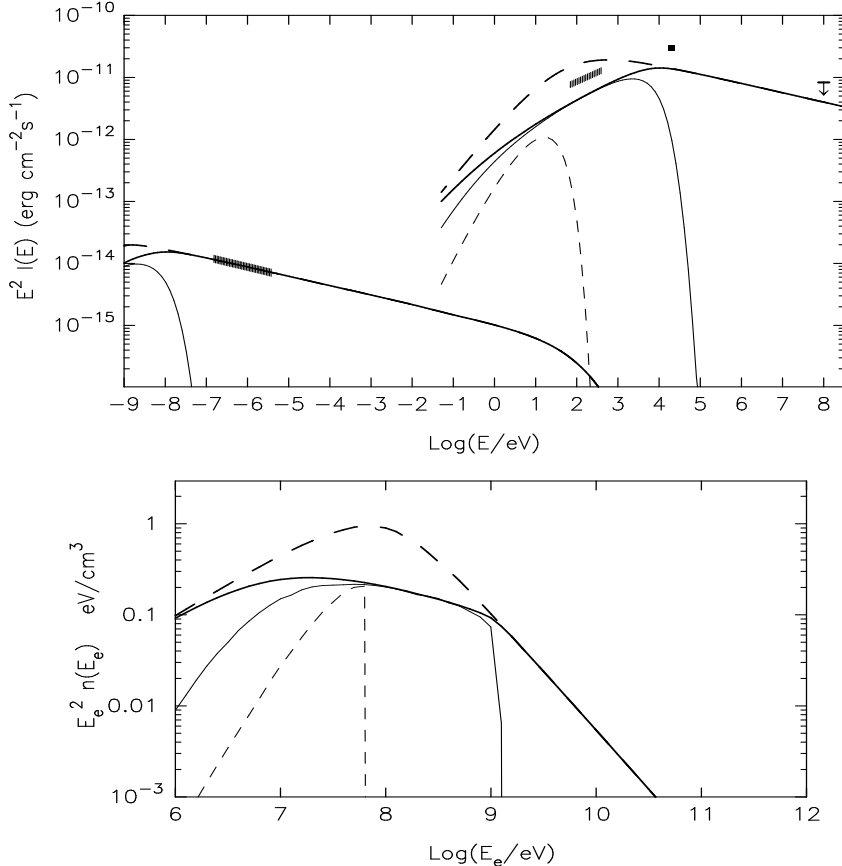


Fig. 3. Synchrotron and IC fluxes (top panel) and the energy distribution of electrons (bottom panel) calculated assuming continuous (heavy lines) and impulsive (thin lines) injection of electrons with $\alpha_{\text{inj}} = 2.3$ and $\gamma_c = 2 \times 10^8$, for the injection times $t = 10^9$ yr (solid) and $t = 10^{10}$ yr (dashed). The ICM gas density $n = 10^{-3} \text{ cm}^{-3}$. For the assumed $B = 0.1 \mu\text{G}$ the electrons are stationarily injected with $L_{\text{inj}} = 2.6 \times 10^{45} \text{ erg/s}$; the total energy input during 1 Gyr is $8.2 \times 10^{62} \text{ erg}$. For the impulsive injection, the same energy inputs as in the corresponding cases of continuous injection are assumed. Nonthermal fluxes from Coma in the radio, EUV, X-ray, and the EGRET upper flux limit (Sreekumar et al. 1996) are also shown.

the value 0.75, in a rather narrow EUV band. After the break, the electron distribution steepens to $\alpha_e = 1 + \alpha_{\text{inj}} = 3.3$, required for the radio emission of Coma.

Such a break in the energy spectrum is necessarily produced by radiative losses of electrons on time scales $\geq 10^9$ yr. Indeed, the characteristic energy loss time in the 2.7 K background radiation field as well as due to synchrotron emission can be written as

$$t_{\text{rad}} = 2.4 \times 10^{12} [C(\gamma) + 0.1 B_{\mu\text{G}}^2]^{-1} \gamma^{-1} \text{ yr} , \quad (1)$$

where $B_{\mu\text{G}} = B/1 \mu\text{G}$. The coefficient $C(\gamma)$ takes into account corrections for the Klein-Nishina effect in the IC energy losses of ultrarelativistic electrons,

which is important for $B \leq 3 \mu\text{G}$. $C(\gamma) = 1$ for $\gamma \ll 10^8$ (IC losses in the Thompson limit), but $C(10^8) \simeq 1/2$, $C(2 \times 10^8) \simeq 1/3$, and $C(5 \times 10^8) \approx 1/6$.

For a magnetic field $\leq 3 \mu\text{G}$ and timescales $\simeq (1 - 3) \times 10^9 \text{ yr}$, equation (1) predicts the radiative cutoff energy $\gamma_{\text{br}} \sim 10^3$. It is important to note that relativistic electrons need to be produced (accelerated) in the ICM *continuously* during all these last years, because in the case of an ‘impulsive’ injection of the electrons the radiative losses would remove all particles with energies above γ_{br} , and then the radio spectra cannot be explained.

This is seen in Fig. 3 which shows the results of calculations that assume both continuous and impulsive injection of electrons with a spectrum

$$Q(\gamma) \propto \gamma^{-\alpha_{\text{inj}}} \exp(-\gamma/\gamma_c), \quad (2)$$

where γ_c defines the assumed characteristic maximum energies of accelerated particles. The fluxes for continuous injection are normalized to the radio flux 2 Jy observed at 400 MHz. The IC radiation for continuous injection during the last $t = 10^9 \text{ yrs}$ (heavy solid line) has the spectral shape of the EUV flux, and for a slightly smaller magnetic field (cf. Fig.4), or an injection time larger by a factor of 2, it can also explain the absolute EUV flux. However in the case of relativistic electron production on much larger time scales, $\sim 10^{10} \text{ yr}$, the explanation of the shape of the EUV radiation becomes problematic even for continuous injection. Moreover, the agreement with observed spectra becomes worse than shown in Fig.3 if we take into account that for cosmological timescales the energy density of the microwave background increases with redshift as $w_{\text{mbr}} \propto T^4(z) \propto (1+z)^4$. Thus, the electrons responsible for the excess EUV radiation, if indeed it has an IC origin, must have been produced continuously during the recent (1-3) Gyrs. This would be the characteristic age of the accretion shocks in the cluster which seem to be the most probable accelerators for the radio emitting electrons.

An IC origin of the excess EUV flux imposes a strong constraint on the magnetic field in Coma. The variation of the IC flux for different magnetic fields are shown in Fig.4 which demonstrates that the lowest consistent magnetic field strength in Coma is equal to $B = 7.5 \times 10^{-8} \text{ G}$. This field could explain also the excess flux observed by *Beppo-SAX* in hard X-rays beyond 25 keV (Fusco-Femiano et al. 1998), that might be due to IC radiation of GeV electrons. The dot-dashed curve in Fig. 4 falls below both the X-ray and the EUV data. However, the assumption of injection for about 5 Gyr shifts the position of the radiative cutoff energy by factor of 5 and increases by the same factor the number of low energy electrons. The number of electrons with $\gamma \sim 300$ is also increased for a steeper injection spectrum, $\alpha_{\text{inj}} = 2.5$. Both these options could marginally explain the radio synchrotron and EUV IC fluxes. Thus an IC origin of the excess EUV radiation restricts the cluster magnetic field to a

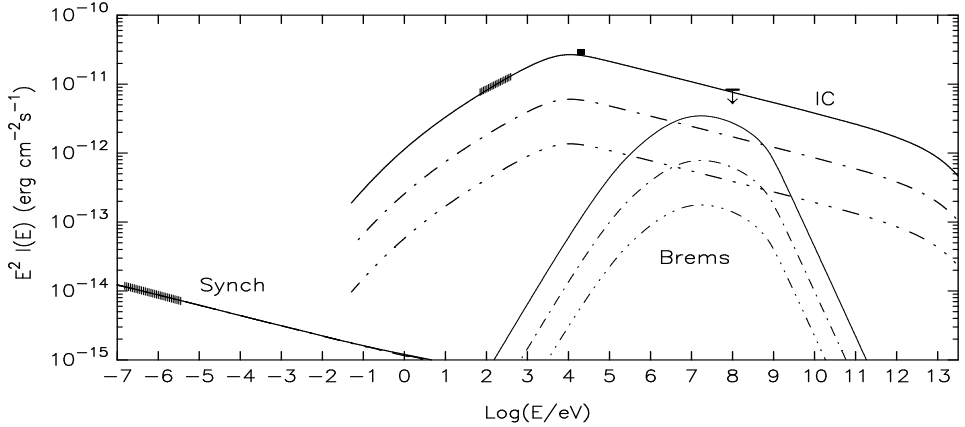


Fig. 4. Nonthermal radiation fluxes calculated for continuous injection of electrons during $t = 10^9$ yr, for different ICM magnetic fields: $B = 7.5 \times 10^{-8}$ G (solid lines), 1.5×10^{-7} G (dot-dashed lines), and 3×10^{-7} G (3-dot-dashed lines)

narrow range around $0.1 \mu\text{G}$.

For magnetic fields $B \simeq 10^{-7}$ G the observed radio fluxes require injection of accelerated particles with a luminosity $L_{\text{inj}} \simeq 3 \times 10^{45}$ erg/s. In a thermal gas with density $n \sim 10^{-3}$ cm $^{-3}$, a *secondary* origin of the relativistic electrons, i.e. their production in pp interactions, would require an enormously large total energy in relativistic protons. Indeed, the luminosity in the $\pi^\pm - \mu^\pm$ -decay electrons can be estimated as

$$L_\pm \simeq 7.7 \times 10^{40} (n_p/10^{-3} \text{ cm}^{-3})^{-3} (E_{\text{CR}}/10^{60} \text{ erg}) \text{ erg/s.} \quad (3)$$

The fluxes of IC gamma-rays to be expected at TeV energies are shown in Fig. 5. for the case of $B = 10^{-7}$ G and acceleration of electrons up to an exponential cutoff energy $E_c = 100$ TeV. For magnetic fields $\sim 0.1 \mu\text{G}$ the diffusive shock acceleration mechanism in the Bohm limit still allows such high values for accelerated electrons. In this limit the acceleration time, defined by the rate $d\gamma/dt \simeq \gamma u^2/D(\gamma)$ where u is the shock speed and $D(\gamma)$ is the diffusion coefficient, is estimated as

$$t_{\text{acc}} \simeq 5.4 \times 10^{-5} u_3^{-2} B_{\mu\text{G}}^{-1} \gamma \text{ yr,} \quad (4)$$

where $u_3 = u/10^3$ km/s. Equating t_{acc} with t_{rad} shows that values $\gamma \geq 10^8$ are possible.

The solid line in Fig. 5 corresponds to the solid curve in Fig. 3. The TeV fluxes of IC γ -rays in that case correspond to several per cent of the TeV emission from the Crab Nebula. In the case of single power law injection with $\alpha_{\text{inj}} = 2.3$ a further increase of the IC fluxes at TeV energies are impossible because of the EGRET upper limit above 100 MeV (Sreekumar et al 1996). Note,

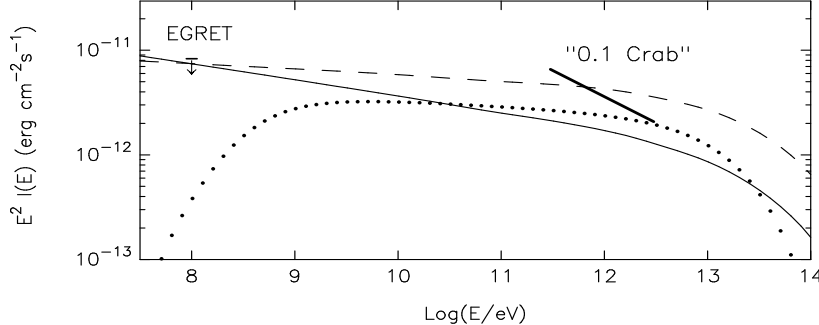


Fig. 5. IC γ -ray fluxes expected from the Coma for $B = 7.5 \times 10^{-8}$ G and $\alpha_{\text{inj}} = 2.3$ (solid lines), and $B = 9 \times 10^{-8}$ G and $\alpha_{\text{inj}} = 2.1$ (dashed lines). The dots show the γ -ray fluxes produced in pp interactions of CRs with $E_{\text{CR}} = 3 \times 10^{62}$ erg in ICM with $n = 10^{-3}$ cm $^{-3}$.

however, that for a more realistic modelling of Coma as a spatially nonuniform source, the power law index α_{inj} could be somewhat smaller than 2.3. We do not consider here this possibility, which should address also the question of different angular sizes of Coma in EUV and radio, as well as the flattening of the radio spectra observed towards the core of the cluster (Giovannini et al. 1993; Deiss et al. 1997). In Fig. 5 the dashed line shows the maximum of the IC radiation fluxes to be expected in the case of $\alpha_{\text{inj}} = 2.1$, which is then at the 0.1 Crab level. The dots correspond to the π^0 -decay fluxes produced by hadronic CRs with $\alpha_{\text{cr}} = 2.1$, assuming $E_{\text{CR}} = 3 \times 10^{62}$ erg. The size of the radio emission produced by high-energy electrons in Coma is about half a degree. Therefore we can expect in that case a similarly large size for the TeV emission. Detection of such extended and weak (≤ 0.1 Crab) TeV fluxes by current instruments is problematic, but they are quite accessible for the future HESS and VERITAS arrays.

These results for the IC fluxes relate to the case of ICM magnetic fields $B \simeq 10^{-7}$ G. However, the estimates for the magnetic fields in Coma range from 0.1 to several μ G. In particular, Kim et al. (1990) and Feretti et al. (1995) deduced magnetic fields $B \simeq 1.7 \mu$ G and $B \simeq 6.0 \mu$ G, respectively, from Faraday rotation measurements on background radio sources. If this is so, then an IC origin of the excess EUV fluxes is absolutely excluded. The only other possibility left for an explanation of this radiation in terms of nonthermal radiation is synchrotron production by very high energy electrons. The interpretation of the steep radio fluxes then requires a second component of nonthermal electrons.

For a production of synchrotron photons with energies 200 eV ($\nu \sim 5 \times 10^{16}$ Hz) in magnetic fields $B \sim 1 \mu$ G one needs electrons with $\gamma \geq 2 \times 10^8$. From Eq.(1), the radiative loss times of these electrons is very short, $t_{\text{rad}} \leq 10^4$ yr. Even assuming a rectilinear propagation of such electrons, the maximum possible distance from the acceleration sites would be less than 3 kpc. Thus, the

acceleration sites of the electrons should be rather smoothly distributed in the ICM in order to result in a smooth distribution of the synchrotron EUV radiation. This seems quite reasonable for accretion shocks, but not for isolated point sources like active galaxies. Another requirement is that the spectrum of accelerated particles should be very hard, with $\alpha_{\text{inj}} \simeq 1.5$. Then the spectrum of electrons steepens to $\alpha_e \simeq 2.5$ which is required for the production of synchrotron radiation with $\alpha_{\text{uv}} \simeq 0.75$.

In Fig. 6 we show the spectra of the synchrotron and IC radiation generated in a magnetic field $B = 2 \mu\text{G}$ by two different populations of relativistic electrons. The dashed curves are produced, as in previous figures, by electrons continuously injected into the ICM during recent epochs up to $t \geq 10^9 \text{ yr}$ with $\alpha_{\text{inj}} = 2.3$ and luminosity $L_{\text{inj}} = 3.5 \times 10^{42} \text{ erg/s}$. For this luminosity, these electrons can be well explained as *secondaries* produced in the interactions of hadronic CRs, of total energy $E_{\text{CR}} = 4.5 \times 10^{61} \text{ erg/s}$, with an ICM gas of density $n_p = 10^{-3} \text{ cm}^{-3}$. They can generate the observed radio emission. On the other hand, the EUV fluxes in Figs. 3 and 4 are produced by the second component with $\gamma_c = 6 \times 10^8$, and a hard injection spectrum with $\alpha_{\text{inj}} = 1$ (solid and dot-dashed curves) and $\alpha_{\text{inj}} = 1.5$ (three-dot-dashed). The curves show that continuous injection of this second component over times exceeding $3 \times 10^7 \text{ yr}$ from now, without reacceleration, would lead to an accumulation of electrons at energies smaller than $\gamma \sim 10^5$. This would be quite sufficient to produce a radio synchrotron flux above the observed level. Moreover, in the case of $\alpha_{\text{inj}} = 1.5$ one has to assume a cutoff in the injection spectrum below $\gamma_{\text{low}} \simeq 10^5$. Otherwise the number of low energy electrons in the injection spectrum would be unacceptably high.

Thus, the scenario with high magnetic fields and nonthermal origin of the excess EUV radiation requires that the second electron component enters a reacceleration cycle at least once in $3 \times 10^7 \text{ year}$. In addition, this component should not contain electrons with low energies. Therefore it cannot be produced by reacceleration of secondary electrons.

In a speculative vain this component could be due to run-away pulsars born with kick velocities $\sim 1000 \text{ km/s}$. Another possibility for the pulsars to appear in the ICM would be that they could be dragged there in the process of galaxy-galaxy collisions. Pulsars produce, at the pulsar wind termination shocks, an electron distribution with a strong deficit of low-energy particles (e.g. Arons 1996). These electrons could be kept at those high energies by entering into frequent reacceleration processes on the accretion shocks in the ICM, and could be thus responsible for the second component.

Reacceleration would not affect the radio electrons if it happened in the central region (see Bowyer and Berghöfer 1998). The signature of the second component would be a rising spectrum of IC γ -rays. Fields below $1 \mu\text{G}$ would even

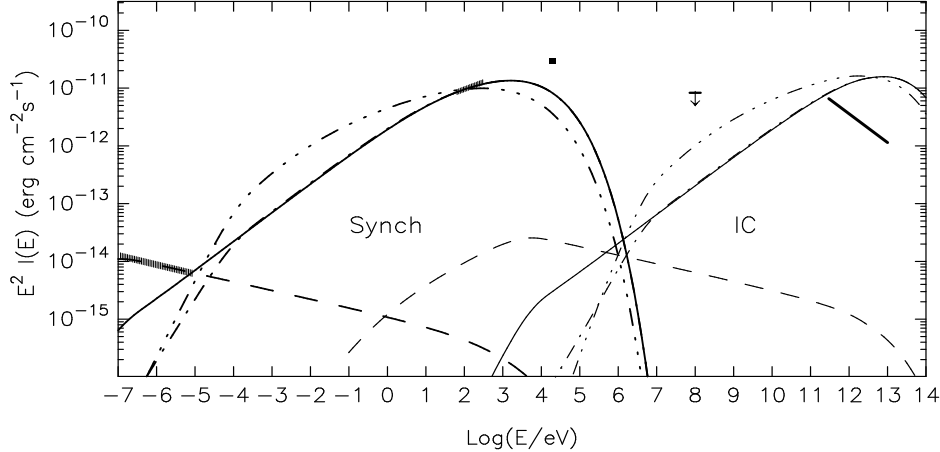


Fig. 6. Nonthermal fluxes expected in the case of $B = 2 \mu\text{G}$ in a two-component model for relativistic electrons in Coma. For the first (radio) component (dashed lines), continuous injection during $t = 10^9 \text{ yr}$ is assumed, with a spectrum of the form of Eq.(2) with $\alpha_{\text{inj}} = 2.3$. For the second (EUV) component the parameters of the continuous injection, without reacceleration of electrons, read: $t = 10^9 \text{ yr}$ and $\alpha_{\text{inj}} = 1$ (solid lines), $t = 3 \times 10^7 \text{ yr}$ and $\alpha_{\text{inj}} = 1$ (dot-dashed), $t = 3 \times 10^7 \text{ yr}$ and $\alpha_{\text{inj}} = 1.5$ (three-dot-dashed). For the case of $\alpha_{\text{inj}} = 1.5$ a rapid transition to $\alpha \propto \gamma^2$ behavior in the injection spectrum in the region $\gamma \leq 10^5$ is assumed. The exponential cutoff energy is $\gamma_c = 6 \times 10^8$, and the gas density is $n = 10^{-3} \text{ cm}^{-3}$. Injection rates for the first and second components are $L_{\text{inj}} = 3.5 \times 10^{42} \text{ erg/s}$ and $L_{\text{inj}} \approx 5.5 \times 10^{44} \text{ erg/s}$, respectively. The total number of electrons in the second component is $N_e \simeq 10^{58}$. The heavy bar corresponds to the "0.1 Crab" flux level.

imply uncomfortably large TeV fluxes from the center of the Coma cluster. Thus the alternative between low and high magnetic fields in the Coma cluster would be given by the shape of the TeV γ -ray spectrum.

Acknowledgements The authors thank F. A. Aharonian and E. N. Parker for illuminating discussions. They also thank H. Böhringer for the permission to use Fig. 1 here.

References

- [1] M. Arnaud, R. Rothenflug, O. Boulade, L. Vigroux, E. Vangioni-Flam, *Astron. Astrophys.* **254** (1992) 49.
- [2] J. Arons, *Space Sci. Reviews* **75** (1996) 235.
- [3] H. Böhringer, in: R. Ekers et al., eds. *Extragalactic Radio Sources 1996* IAU, 357.
- [4] V.S. Berezinsky, P. Blasi, V.S. Ptuskin, *Astrophys. J.* **487** (1997) 529.
- [5] S. Bowyer, T.W. Berghöfer, *Astrophys. J.* **505** (1998) 502.

- [6] D. Breitschwerdt, J.F. McKenzie, H.J. Völk, *Astron. Astrophys.* **269** (1993) 54.
- [7] D. Breitschwerdt, Habilitationschrift, Univ. Heidelberg (1994) 158.
- [8] A.H. Bridle, C.R. Purton, *Astron. J.* **73** (1968) 8.
- [9] B.M. Deiss, *Astron. Astrophys.* **325** (1997) 74.
- [10] T.A. Enßlin, P.L. Biermann, *Astron. Astrophys.* **330** (1998) 90.
- [11] T.A. Enßlin, P.L. Biermann, P.P. Kronberg, X.-P. Wu, *Astrophys. J.* **477** (1997) 560.
- [12] L. Feretti, D. Dallacasa, G. Giovannini, A. Tagliani, *Astron. Astrophys.* **302** (1995) 680.
- [13] R. Fusco-Femiano, D. Dal Fiume, L. Feretti, G. Giovannini, G. Matt, S. Molendi, *astro-ph/9808012* (1998).
- [14] V.L. Ginzburg, *Theoretical Physics and Astrophysics*. Pergamon Press, Oxford, 1979.
- [15] G. Giovannini, et al., *Astrophys. J.* **406** (1993) 399.
- [16] P.A. Henning, *Astron. J.* **97** (1989) 1561.
- [17] C.-Y. Hwang, *Science* **278** (1997) 1917.
- [18] K.-T. Kim, P.P. Kronberg, P.E. Dewdney, T.L. Landecker, *ApJ* **355** (1990) 29.
- [19] P.P. Kronberg, *Rep. Prog. Phys.* **57** (1994) 325.
- [20] R. Lieu, W.-H. Ip, W.I. Axford, M. Bonamente, *astro-ph/9809175* (1998).
- [21] J.P.D. Mittaz, R. Lieu, F.J. Lockman, *Astrophys. J.* **498** (1997) L17.
- [22] E.N. Parker, *Astrophys. J.* **401** (1992) 137.
- [23] V.S. Ptuskin, H.J. Völk, V.N. Zirakashvili, D. Breitschwerdt, *Astron. Astrophys.* **321** (1997) 434.
- [24] R. Schaaf, W. Pietsch, P.L. Biermann, P.P. Kronberg, T. Schmutzler, *Astrophys. J.* **336** (1989) 722.
- [25] R. Schlickeiser, A. Sievers, H. Thiemann, *Astron. Astrophys.* **182** (1987) 21.
- [26] P. Sreekumar, et al., *Astrophys. J.* **464** (1996) 628.
- [27] M. Steinmetz, PhD thesis, Technische Universität München (1993).
- [28] H.J. Völk, F.A. Aharonian, D. Breitschwerdt, *Space Sci. Rev.* **75** (1996) 279. (Paper I)
- [29] D.A. White, A.C. Fabian, *Mon. Not. R. Astron. Soc.* **273** (1995) 72.
- [30] V.N. Zirakashvili, D. Breitschwerdt, V.S. Ptuskin, H.J. Völk, *Astron. Astrophys.* **311** (1996) 113.